Optics Communications 285 (2012) 2558–2562

Contents lists available at SciVerse ScienceDirect

Optics Communications

journal homepage: www.elsevier.com/locate/optcom

Systematical research on the characteristics of a vertical coupled Fabry–Perot plasmonic filter

Lin Liu, Xia Hao *, Yutang Ye, Juanxiu Liu, Zhenlong Chen, Yuncen Song, Ying Luo, Jing Zhang, Liang Tan

School of Opto-electronic Information, University of Electronic Science and Technology of China, 610054, China

ARTICLE INFO

Article history:
Received 10 August 2011
Accepted 30 January 2012
Available online 12 February 2012

Keywords:
Surface plasmon polariton
Filter
Fabry–Perot

ABSTRACT

A nanometric surface plasmon polariton (SPP) filter based on a vertical coupled metal–insulator–metal (MIM) Fabry–Perot resonator is proposed and analyzed. The transmission characteristics of the SPP filter are analyzed in detail by using the finite difference time domain method. And the resonance condition derived by the numerical method is consonant with the analytic model based on the Fabry–Perot model, which includes the metal loss and dispersion effects. And the simulation results show that multiple transmission dips can be formed and the resonance wavelengths of the transmission dips can be altered by the Fabry–Perot cavity length and width. Also the extinction ratio and the quality factor of the filter are affected by the barrier thickness of the coupling region. The proposed nanometric plasmonic filter is simple and very promising for the SPP waveguides platform.

© 2012 Elsevier B.V. All rights reserved.

1. Introduction

Surface plasmon polaritons (SPP) are electromagnetic waves coherently coupled to electron oscillations and propagating at the interface between a dielectric and a metal, evanescently confined in the perpendicular direction [1,2]. When two metal/insulator interfaces are close to each other enough, the SPP waves at the two interfaces are coupled and the metal/insulator/metal (MIM) SPP waveguide can be formed [3,4]. The MIM SPP waveguide is very promising for the optical signal propagation and processing in future high density integration platform because it can break through the diffraction limit and achieve nanometric mode size, which cannot be realized by the traditional dielectric waveguides. And both the optical and electric signals can be propagated through the SPP waveguides while the dielectric waveguides can only guide optical signals. So the MIM SPP waveguide components have been one kind of research hotspots in the plasmonics domain. Until now, different SPP waveguide components based on the MIM structure have been demonstrated, such as bends and splitters [5,6], Mach–Zehnder interferometers [7], Y-shaped combiners [8] and so on. Because the SPP waveguide filter is very important for the SPP integration platform, various types of the MIM SPP filters have been proposed, which include the Bragg grating filters [9–11], ring resonator filters [12–16], tooth shaped filters [17,18]. Recently, a subwavelength MIM SPP filter with side coupled Fabry–Perot (F–P) cavity has been proposed [19]. But just as the author states, the side coupled SPP filter has the disadvantage that the filtering spectra of the SPP filter will be distorted badly by decreasing the barrier gap size. In order to overcome this shortcoming, in this article we propose a MIM SPP filter which composes a vertical coupled MIM F–P cavity, whose filtering spectra are not distorted by the barrier gap size. This may give much more flexibility for the device fabrication. The transmission characteristics of the proposed SPP filters are investigated by the finite difference time domain (FDTD) method, with perfect matching layer absorbing boundary conditions. Also the analytic method based on the Fabry–Perot model, which includes the metal loss and dispersion effects is introduced to explain the filtering mechanism qualitatively, which is consistent with the FDTD results. And the simulation results show that multiple transmission dips can be formed and the resonance wavelengths of the dips can be altered by the Fabry–Perot cavity length and width. The extinction ratio and the quality factor of the filter are affected by the barrier thickness of the coupling region. Also the quality factors of this SPP filters are better than those of the tooth shape filters [17].

2. The structure and the transmission characteristics of the SPP filter

2.1. The vertical coupled F–P SPP filter structure and the FDTD simulation method

Fig. 1(a) shows the schematic of the proposed SPP filter, which is made up of the MIM waveguides. The truncate MIM waveguide, which forms an F–P cavity, is vertical coupled to the bus MIM waveguide. The widths of the bus MIM waveguide and the F–P cavity are w_1 and w_2, respectively. And L and g are the F–P cavity length and

* Corresponding author. Tel.: +86 15881089342.
E-mail address: angle13317224012@163.com (X. Hao).

0030-4018/$ – see front matter © 2012 Elsevier B.V. All rights reserved.
doi:10.1016/j.optcom.2012.01.066

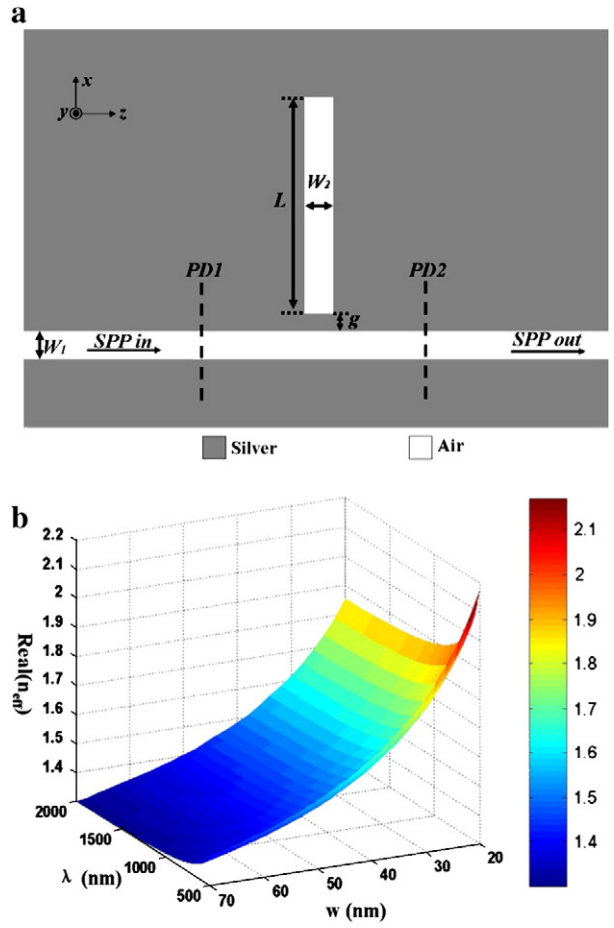

Fig. 1. (a) The schematic of the proposed vertical coupled F–P SPP filter. (b) The dependence of Re(n_{eff}) of the fundamental TM mode on the wavelength λ and the MIM waveguide width w.

the barrier thickness of the coupling region. Here the metal and insulator are silver and air, respectively. Because the MIM waveguides are the basic units of the proposed SPP filter and only the transverse magnetic (TM) mode can be supported by the MIM waveguide, the real part of the effective index (Re(n_{eff})) of the fundamental TM mode is calculated and plotted by the dispersion relation [17]:

$$\varepsilon_{in}k_{z2}+\varepsilon_m k_{z1}\coth\left(-\frac{ik_{z1}}{2}d\right)=0 \tag{1}$$

And k_{z1} and k_{z2} are

$$k_{z1}^2=\varepsilon_{in}k_0^2-\beta^2,\ k_{z2}^2=\varepsilon_m k_0^2-\beta^2 \tag{2}$$

Where ε_{in}, ε_m are the dielectric constants of the insulator and the metal, $k_0=2\pi/\lambda$ is the free-space wave vector. And the dielectric constant of the metal silver is characterized by the Lorentz–Drude model [15,20]:

$$\varepsilon_m=\varepsilon_\infty-\sum_{m=0}^{5}\frac{G_m\Omega_m^2}{\omega_m^2-\omega^2+i\omega\Gamma_m} \tag{3}$$

Where ε_∞ is the relative permittivity in the infinity frequency, G_m is the oscillator strengths, Ω_m is the plasma frequency, ω is the angular frequency of incident light, and all these parameters used in the simulations are the same as in Ref. [18]. From Fig. 1(b), it is clear that Re(n_{eff}) increases when the incident wavelength or the waveguide width decreases. And the effect of the waveguide width on the Re(n_{eff}) is much greater than that of the incident wavelength.

In order to study the characteristics of the proposed SPP filter, the 2D FDTD method with the perfect matched layer boundary condition is used to calculate the transmission spectra. The fundamental TM mode of the MIM waveguide is excited by a pulse source and the mesh grid size is set to be 1 nm in order to keep convergence. As shown in Fig. 1(a), the power monitor PD_1 is set to detect the incident power (without the F–P resonator as the reference) and the power monitor PD_2 is set to detect the transmission power (with the F–P resonator as the filter). And the transmittance is defined as $T=B/A$ [16].

2.2. The resonance condition of the vertical coupled F–P SPP filter

Because the proposed vertical coupled F–P SPP filter is made of metal and with the cavity length on the order of the wavelength, the metal loss, dispersion of the MIM waveguides and the penetration depths at the two ends of the F–P cavity must be considered to get the resonance condition accurately. As the conventional Fabry–Perot model, the resonance condition (phase matching condition) for the F–P resonator is $\varphi=2\cdot N\pi$ (N = 1, 2, 3…), where φ is the phase difference of a round trip of the effective cavity length L_{eff} of the F–P cavity:

$$\varphi=(2\pi/\lambda)\times 2\times L_{eff} \tag{4}$$

$$L_{eff}=n_{eff}\times L+L_{pen1}+L_{pen2} \tag{5}$$

Where L_{pen1} and L_{pen2} are the penetration depths at the two ends of the F–P cavity. And the penetrate depth can be given as [21]:

$$L_{pen}=L_{pen1}=L_{pen2}=[\lambda(\pi-\phi)]/(4\pi) \tag{6}$$

Where the phase shift on reflection is given by

$$\phi=\arctan\left(\frac{2n_0k_1}{n_0^2-n_1^2-k_1^2}\right) \tag{7}$$

And $n_0=1$, $n_{Ag}=n_1-ik_1$ are the refractive indices of air and Ag, respectively. By combing Eqs. (4) and (5), the following phase matching condition can be deduced:

$$2\cdot\left(n_{eff}\times L+2\cdot L_{pen}\right)=N\cdot\lambda \quad (N=1,2,3\ldots) \tag{8}$$

When $L=500nm$, $w_1=w_2=50nm$, $g=10nm$, the Eq. (8) can be resolved by the graphic approach as shown in Fig. 2(a). The resonance wavelengths can be found as the intersection points shown in Fig. 2(a). In order to examine the correctness of the resonance condition, the transmission spectrum of the vertical coupled F–P SPP filter is also calculated by the FDTD method and shown in Fig. 2(b). The results show that the three resonance wavelengths in Fig. 2(a) are consistent with those in Fig. 2(b) well.

2.3. The structure parameters' effects on the vertical coupled F–P SPP filter

Just as the dielectric waveguide F–P filter, the resonance wavelength of the proposed vertical coupled F–P SPP filter can be altered by changing the F–P cavity length. Fig. 3(a) shows the transmission spectra of the SPP filter with three F–P cavity length of $L=300nm$, $400nm$, $500nm$. And the resonance wavelengths with various F–P cavity lengths are calculated and shown in Fig. 3(b). It is obvious that the resonance wavelength of the F–P SPP filter can be linear changed by altering the resonant cavity lengths. Also the slope of the 1st (N = 1) resonance is larger than that of the 2nd (N = 2) resonance.

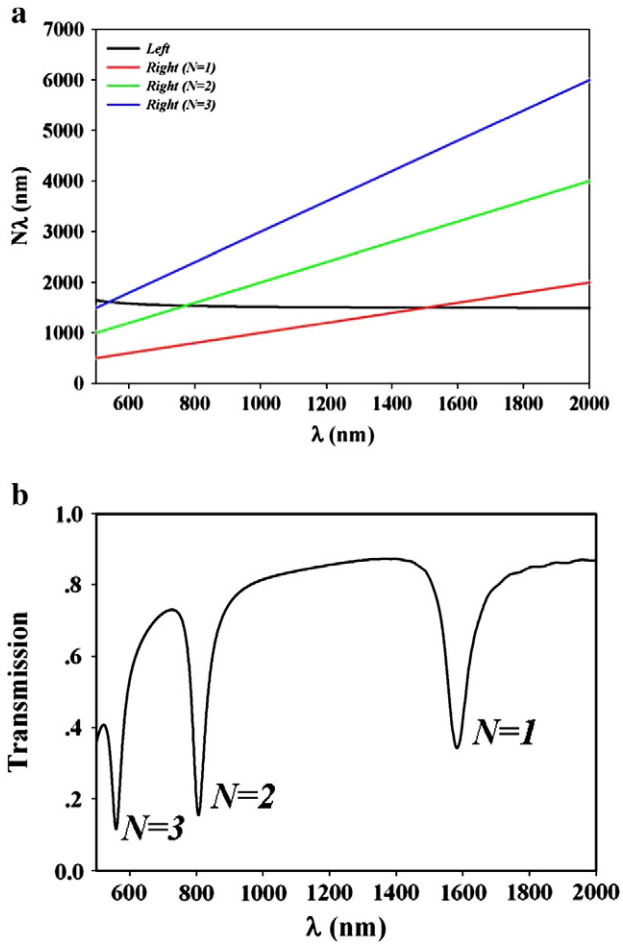

Fig. 2. (a) The resonance wavelength resolved by the graphic approach. (b) The transmission spectrum of the vertical coupled F–P SPP filter simulated by the FDTD method ($w_1 = w_2 = 50$ nm, L = 500 nm, g = 10 nm).

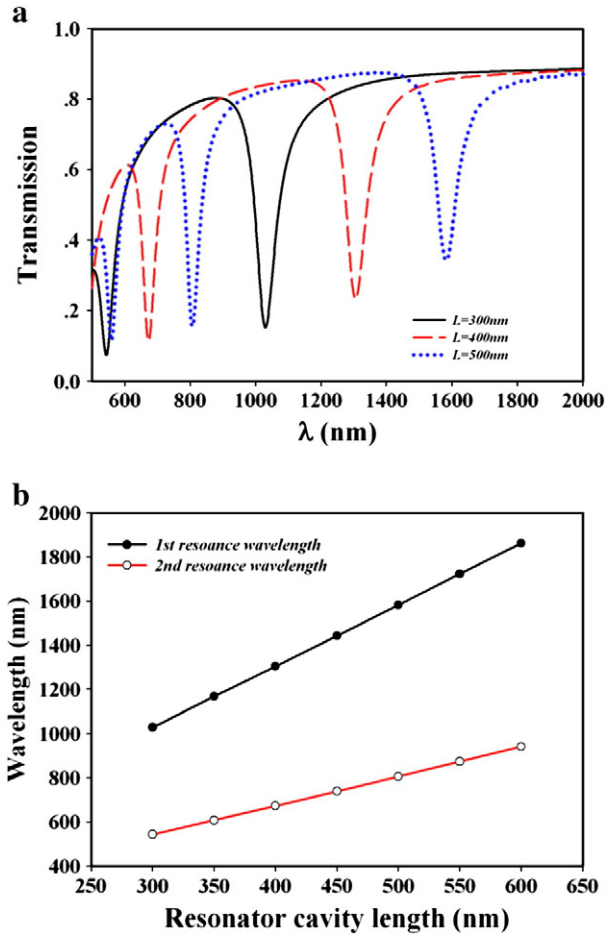

Fig. 3. (a) The transmission spectra of the vertical coupled F–P SPP filter with different L ($w_1 = w_2 = 50$ nm, g = 10 nm). (b) The 1st and 2nd resonance wavelengths of the transmission dips as function of the cavity lengths.

Because the barrier thickness g of the coupling region which determines the coupling strength is very important to the filtering characteristics, the transmission spectra of the vertical coupled F–P SPP filters with different barrier thickness are simulated and shown in Fig. 4(a). Also the transmission spectra of the side coupled SPP filter with different barrier thickness are plotted as Fig. 4(b) to compare with the vertical coupled F–P SPP filter. As Ref. [19] states, the side coupled SPP filter has the disadvantage that the transmission spectra of the SPP filter will be distorted badly by decreasing the barrier gap size. This is because the coupling length of the side coupled SPP filter is larger than one period with increasing the coupling strength when the barrier thickness is decreased. But as shown in Fig. 4(a), the proposed vertical coupled F–P SPP filter can overcome this shortcoming and it's transmission spectrum is not distorted with the altering barrier thickness. And from Fig. 4(a), it is obvious that the extinction ration of the SPP filter is decreased with increasing barrier thickness. This is because the coupling strength is decreased and less SPP energy is coupled into the F–P cavity by increasing the barrier thickness. Also the resonance wavelength is little increased with decreasing barrier thickness because the effective index of the MIM waveguide mode can be altered by the barrier thickness in the coupling region. And when the barrier thickness is reduced to zero, the proposed vertical coupled F–P SPP filter is evolved to the tooth shape SPP filter [17]. It is obvious that the quality factor (Q value) of the vertical coupled F–P filter is decreased with decreasing barrier thickness, and it has larger quality factor than the tooth shape SPP filter. For example, the quality factors of the 2nd resonance with the barrier thickness g = 20 nm, 10 nm, 5 nm, 0 nm are about Q = 28, 16.4, 9.2, 5.1, respectively. The |Hy| field distributions at the 1st and 2nd resonances (1692 nm and 847 nm) are shown in Fig. 4(c, d). It is obvious that when the resonance conditions of $L = \lambda_{spp}$, $L = 2\lambda_{spp}$ are satisfied, standing-wave patterns can be formed in the resonant cavity and transmission dips are formed.

Also the resonance wavelength and the extinction ratio of the vertical coupled F–P SPP filter can be altered by the width of the F–P cavity. Fig. 5 shows the transmission spectra of the SPP filter with different cavity width w_2. The resonance wavelength is shifted to the short wavelength when w_2 increases. This is because the $Re(n_{eff})$ of the MIM waveguide is decreased by increasing w_2 according to Fig. 1(b). And the extinction ratio can be increased by increasing w_2, because more SPP energy could be coupled into the F–P cavity by increasing the coupling length, which is equal to w_2.

At last, the resonance SPP wave can be coupled out by adding another MIM waveguide just as shown in Fig. 6(a). Fig. 6(b) shows the transmission and drop spectra of the SPP filter. It is clear that when resonance occurs, the SPP wave is filtered at the transmission port while partly coupled out at the drop port. And the resonance wavelength, drop efficiency, and extinction ratio can also be adjusted by altering the structure parameters.

3. Conclusion

In this article, a nanometric SPP filter based on vertical coupled F–P cavity is proposed and investigated. The resonance wavelengths,

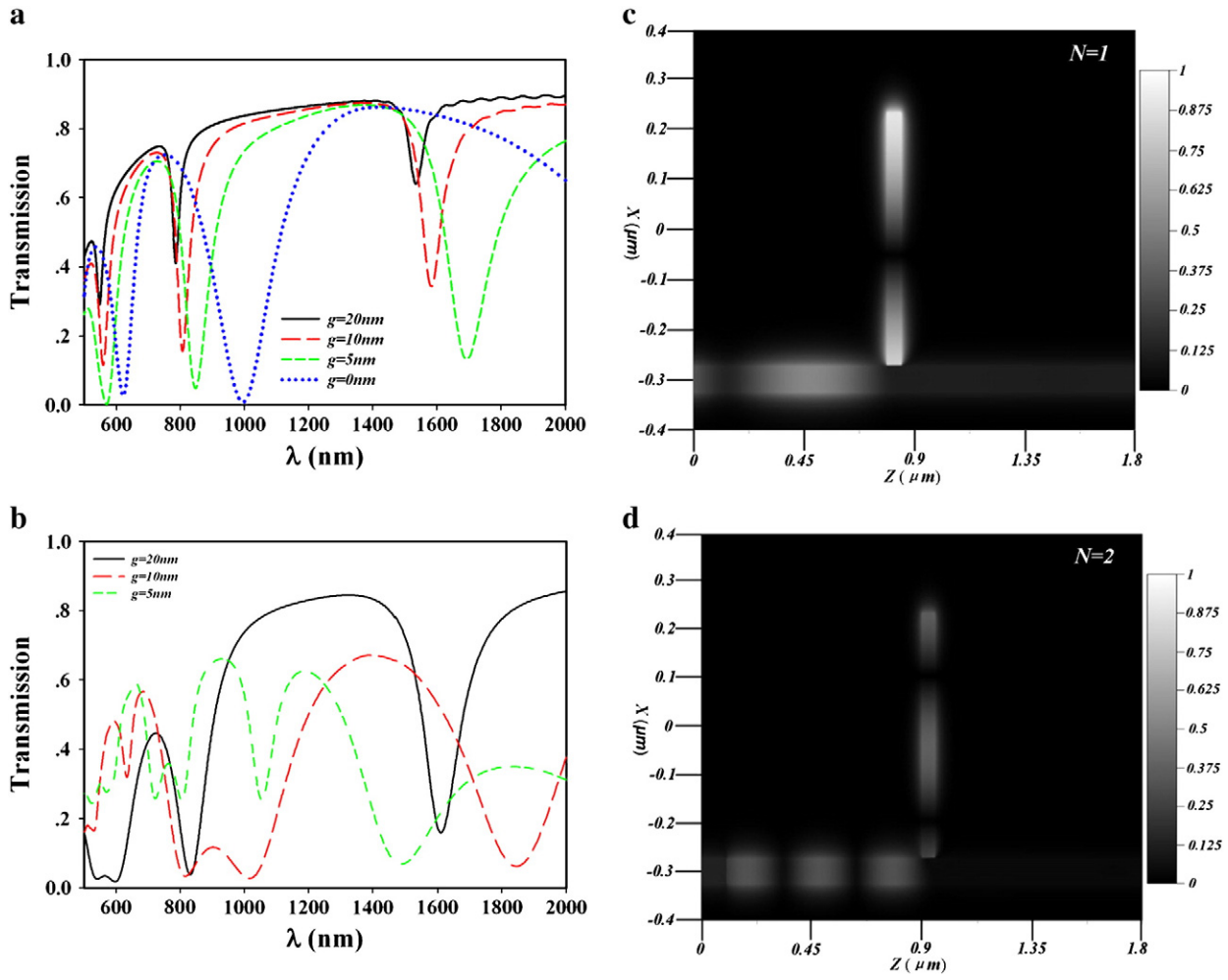

Fig. 4. (a) The transmission spectra of the vertical coupled F–P SPP filter with different barrier thickness g ($w_1 = w_2 = 50$ nm, L = 500 nm). (b) The transmission spectra of the side coupled SPP filter with different barrier thickness g ($w_1 = w_2 = 50$ nm, L = 500 nm). (c, d) The $|H_y|$ field patterns of the SPP filter at the 1st and 2nd resonances ($w_1 = w_2 = 50$ nm, L = 500 nm, g = 5 nm).

field profiles, extinction ratios and the quality factors of the SPP filters are analyzed. Also the resonance condition is derived by the phase match condition of the F–P cavity model, which consists with the numerical FDTD results. The results show that multiple resonances could be realized and the standing wave can be realized in the F–P cavities. And the resonance wavelength of the F–P SPP filter can be linearly changed by altering the resonant cavity lengths. The extinction ration of the SPP filter is decreased with increasing barrier thickness while the quality factor of the SPP filter is decreased with decreasing barrier thickness. In conclusion, the proposed vertical coupled F–P SPP filter is very promising for high density SPP waveguide integrations.

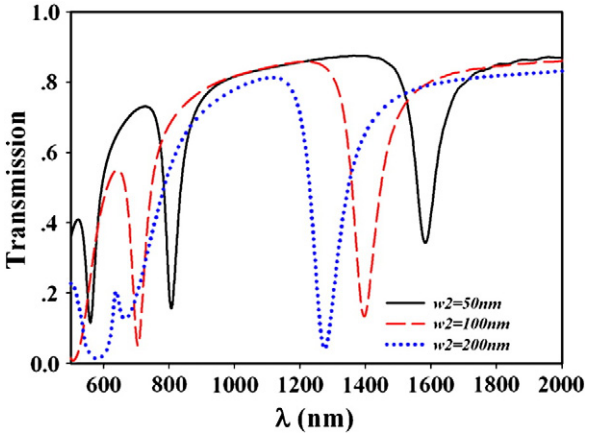

Fig. 5. The transmission spectra of the vertical coupled F–P SPP filter with different w_2 ($w_1 = 50$ nm, g = 10 nm, L = 500 nm).

References

[1] William L. Barnes, Alain Dereux, Thomas W. Ebbesen, Nature 124 (14) (2003) 824.
[2] Ekmel Ozbay, Science 311 (13) (2006) 189.
[3] Sergey I. Bozhevolnyi, Valentyn S. Volkov, Eloise Devaux, Jean-Yves Laluet, Thomas W. Ebbesen, Nature 440 (23) (2006) 508.
[4] Sergey I. Bozhevolnyi, Valentyn S. Volkov, Eloise Devaux, Thomas W. Ebbesen, Physical Review Letters 9 (5) (2005) 046802.
[5] Georgios Veronis, Shanhui Fan, Applied Physics Letters 8 (7) (2005) 131102.
[6] Tae-Woo Lee, Stephen K. Gray, Optics Express 13 (24) (2005) 9652.
[7] Zhanghua Han, Liu Liu, Erik Forsberg, Optics Communication 259 (2006) 690.
[8] Hongtao Gao, Haofei Shi, Changtao Wang, Chunlei Du, Xiangang Luo, Qiling Deng, Yaoguang Lv, Xiangdi Lin, Hanmin Yao, Optics Express 13 (26) (2005) 10795.
[9] Amir Hosseini, Yehia Massoud, Optics Express 14 (23) (2006) 11318.
[10] Jian-Qiang Liu, Ling-Ling Wang, Meng-Dong He, Wei-Qing Huang, Dianyuan Wang, B.S. Zou, Shuangchun Wen, Optics Express 16 (7) (2008) 4888.
[11] Yongkang Gong, Leiran Wang, Xiaohong Hu, Xiaohui Li, Xueming Liu, Optics Express 17 (16) (2009) 13727.
[12] Sanshui Xiao, Liu Liu, Min Qiu, Optics Express 14 (7) (2006) 2932.
[13] Amir Hosseini, Yehia Massoud, Applied Physics Letters 9 (2007) 181102.
[14] Jianlong Liu, Guangyu Fang, Haifa Zhao, Yan Zhang, Shutian Liu, Journal of Physics D 4 (3) (2010) 055103.

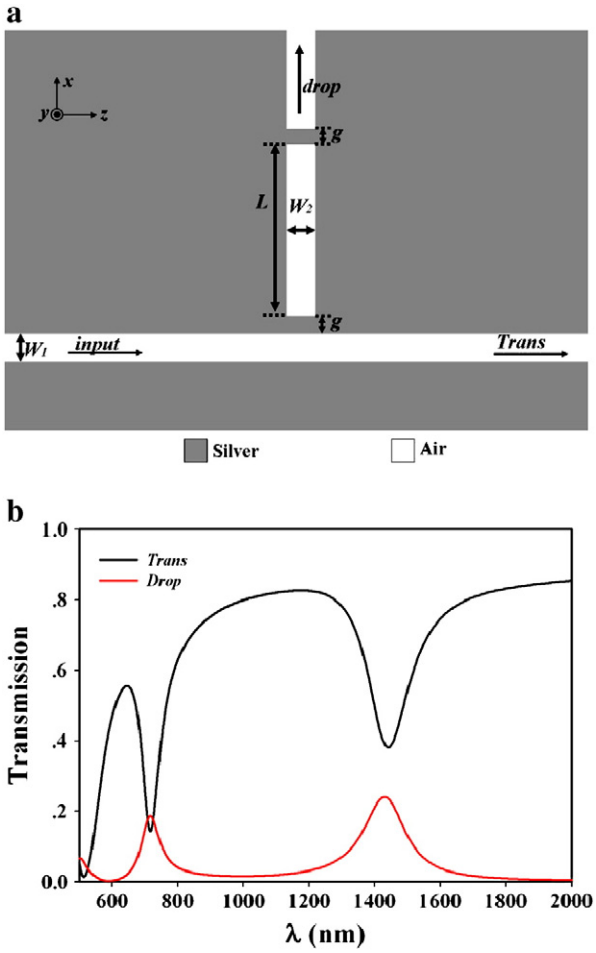

Fig. 6. (a) The schematic of the vertical coupled F–P SPP filter with drop port. (b) The transmission and drop spectra of the SPP filter ($w_1 = 50$ nm, $w_2 = 100$ nm, $L = 500$ nm, $g = 10$ nm).

[15] Tong-Biao Wang, Xie-Wen Wen, Cheng-Ping Yin, He-Zhou Wang, Optics Express 17 (26) (2009) 24096.
[16] Binfeng Yun, Guohua Hu, Yiping Cui, Journal of Physics D: Applied Physics 4 (3) (2010) 385102.
[17] Xian-Shi Lin, Xu-Guang Huang, Optics Letters 33 (23) (2008) 2874.
[18] Jin Tao, Xuguang Huang, Xianshi Lin, Jihuan Chen, Qin Zhang, Xiaoping Jin, Journal of the Optical Society of America B 27 (2) (2010) 323.
[19] Qin Zhang, Xuguang Huang, Xianshi Lin, Jin Tao, Xiaoping Jin, Optics Express 17 (9) (2009) 7549.
[20] A.D. Rakic, A.B. Djurisic, J.M. Elazar, M.L. Majewski, Applied Optics 37 (22) (1998) 5271.
[21] Fengying Ma, Xingyuan Liu, Applied Optics 46 (25) (2007) 6247.